

Ab initio thermodynamics and phase diagram of solid magnesium: A comparison of the LDA and GGA

S. Mehta^{a)}

Atomic Weapons Establishment, Aldermaston, Reading, Berkshire RG7 4PR, United Kingdom

G. D. Price

Department of Earth Sciences, University College London, London WC1E 6BT, United Kingdom

D. Alfè

Department of Earth Sciences, University College London, London WC1E 6BT, United Kingdom

and Department of Physics and Astronomy, University College London, London WC1E 6BT,

United Kingdom

(Received 7 March 2006; accepted 4 October 2006; published online 16 November 2006)

The finite temperature density functional theory and quasiharmonic lattice dynamics have been used to compute numerous thermodynamic properties of hexagonal close packed magnesium using both the local density approximation (LDA) and the generalized gradient approximation (GGA) for the exchange-correlation potential. Generally, it is found that there exist only minor differences between the LDA and GGA computed properties, with both giving good agreement with experiment. The hcp-bcc phase boundary has also been computed and is found to be in agreement with experimental observation. Again, only slight differences are found between the LDA and GGA.

[DOI: [10.1063/1.2374892](https://doi.org/10.1063/1.2374892)]

I. INTRODUCTION

As is well known, the only necessary approximation required in the density functional theory^{1,2} is the exchange-correlation potential. The two most commonly used are the local density approximation (LDA) and the generalized gradient approximation (GGA). The LDA is known to overbind materials and as a result predicts cohesive energies, equilibrium bulk moduli that are too large, and equilibrium lattice parameters that are too small. In principle, the GGA is an improvement upon the LDA. In practice, however, it does not necessarily lead to improved results. Studies performed on various elements^{3,4} find that the GGA generally tends to produce better cohesive energies but can overcorrect bulk moduli and lattice parameters to the extent that the agreement is worse than the LDA. Despite such examinations, it does not appear possible to determine *a priori* which approximation for the exchange-correlation potential should be used for a given material.

Favot and Dal Corso⁵ suggest that a GGA functional should not be judged solely on its ability to reproduce equilibrium structural parameters, since good agreement for such quantities does not always guarantee accurate phonon dispersions. In their work, phonon dispersion spectra were computed for a number of elements at the experimental equilibrium volume, and they found that the GGA systematically gave lower phonon frequencies than the LDA. In comparison with experiment, the GGA calculations fell in to all the possible categories: producing spectra with accuracies that were better, worse, or similar to those obtained from the LDA.

Phonon spectra are a key ingredient in the calculation of

the thermal properties of a solid. A detailed study which compared the performance of the LDA and GGA in calculating the thermal properties of copper was performed by Narasimhan and de Gironcoli.⁶ They computed a number of thermodynamic properties at atmospheric pressure as a function of temperature. Generally, it was found that the experimental results lay in between the GGA and LDA calculations, with both approximations giving similar accuracy.

Since the free energy differences between competing crystal structures is very small, an accurate computation of solid-solid phase boundaries is a particularly challenging task. The question naturally arises as to the performance of the exchange-correlation functionals in the calculation of phase diagrams. Studies performed on cold systems, for example, Refs. 7 and 8, find that the LDA produces transition pressures that are too low with respect to experimental values and that the GGA tends to improve agreement by predicting larger transition pressures than the LDA.

However, detailed studies comparing the performance of the LDA and GGA in the computation of thermodynamic properties, including phase diagrams, over wide pressure and temperature ranges remain scarce. In this paper, as a step towards addressing this situation, we report on detailed density functional calculations of the thermodynamic properties of magnesium using both the LDA and GGA.

A detailed LDA investigation of magnesium has previously been performed using the generalized pseudopotential theory (GPT): Althoff *et al.*⁹ computed a number of thermodynamic properties of hcp magnesium and found very good agreement with experiment. They also computed the hcp-bcc boundary in the pressure range of 28–52 GPa and their predicted transition pressure at room temperature of 48 GPa is in very good agreement with the experimental value of

^{a)}Electronic mail: s.mehta@awe.co.uk

50 GPa.¹⁰ In a subsequent paper, Moriarty and Althoff¹¹ computed the melt curve and extended the calculation of hcp-bcc boundary to lower pressures and found that it met the melt curve at around 4 GPa. Recently, Errandonea *et al.*¹² probed the low pressure solid phase diagram experimentally and found disagreements with the calculations reported in Ref. 11. It is thus particularly interesting to compare these new experimental results with a prediction of the hcp-bcc phase boundary originating from a different first principles method.

The next section outlines the calculational techniques employed in this work. Section III presents the results of the thermodynamic properties of hcp magnesium. The calculation of the hcp-bcc phase boundary line is reported in Sec. IV. Finally, Sec. V summarizes the paper.

II. METHODOLOGY

In this work it is assumed that the Helmholtz free energy $F(V, T)$ of the system can be written as the sum of two terms,

$$F(V, T) = F_e(V, T) + F_i(V, T), \quad (1)$$

where F_e and F_i are the electronic and ionic Helmholtz free energies, respectively, V is the volume, and T is the temperature.

The electronic free energy was calculated using the projector augmented wave (PAW) implementation of the density functional theory^{13,14} using the Vienna *ab initio* simulation package (VASP).¹⁵ For the exchange-correlation potential, the PW91 (Refs. 16 and 17) functional was used in the GGA calculations and the parametrization of the results of Ceperley and Alder¹⁸ by Perdew and Zunger¹⁹ in the LDA calculations. The PAW potentials used were those supplied with the code and treated the $2p$ and $3s$ electrons as valence states. In the calculation of the electronic free energy, the thermal excitation was treated with the finite temperature density functional method of Mermin.²⁰ Integration over the Brillouin zone was performed using uniform k -point grids. The ionic component of the Helmholtz free energy was computed via the small displacement method within the quasi-harmonic approximation.^{21–24} In this scheme, supercells are first constructed from the primitive cells of the lattice. Small displacements are then given to the atoms in the primitive cell. An approximate force constant matrix is then constructed from the forces induced on all the atoms in the supercell. Next, the dynamical matrix is computed at any arbitrary phonon wave vector as the lattice Fourier transform of the force constant matrix divided by the mass of the atoms. Finally, the square root of the eigenvalues of the dynamical matrix are the phonon frequencies $\{\omega_{\mathbf{q}s}\}$. The ionic free energy can then be computed from the sum²⁵

$$F_i(V, T) = \sum_s \sum_{\mathbf{q}} \frac{1}{2} \hbar \omega_{\mathbf{q}s} + k_B T \ln[1 - \exp(-\hbar \omega_{\mathbf{q}s}/k_B T)], \quad (2)$$

where sums are over phonon wave vectors \mathbf{q} and branches s .

The inevitable noise present in the *ab initio* free energy makes it unsuitable for use directly in the computation of thermodynamic quantities. Instead, it is usual to obtain an

analytic representation of the *ab initio* results. In this work the electronic and ionic free energies were parametrized separately. The electronic free energy was parametrized, following the method detailed in Ref. 24. In this scheme each electronic free energy isotherm is first fitted to the third-order Birch-Murnaghan equation of state²⁶

$$F_e(V, T) = \frac{3}{4} K_0 V_0 x^2 \left(\eta x + \frac{3}{2} \right) + F_0, \quad (3)$$

where $x = [(V_0/V)^{2/3} - 1]$ and $\eta = \frac{3}{4}(K'_0 - 4)$. This process yields the bulk modulus K_0 , its derivative with respect to pressure K'_0 , and the free energy F_0 at the equilibrium volume V_0 . The temperature dependence of each these quantities is then parametrized by fitting to polynomials in T ,

$$K_0(T) = \sum_{i=0}^n k_{0i} T^i, \quad K'_0(T) = \sum_{i=0}^n k'_{0i} T^i, \quad (4)$$

$$V_0(T) = \sum_{i=0}^n v_{0i} T^i, \quad F_0(T) = \sum_{i=0}^n f_{0i} T^i.$$

The ionic free energy is more awkward to parametrize. The authors of Ref. 24 employed the high temperature expansion of the partition function for this purpose, as they were interested in melting properties. However, this representation omits the zero point energy of the lattice. Since this quantity could have an effect on the computed solid-solid phase boundary, particularly in the high-pressure–low-temperature region, we fitted the ionic free energy to the Einstein function

$$F_i(V, T) = \frac{3}{2} k \theta_E(V, T) + 3kT \ln[1 - \exp(-\theta_E(V, T)/T)]. \quad (5)$$

For each free energy isotherm, Eq. (5) was solved to determine the Einstein temperature θ_E , as a function of V . The resulting θ_E - V relation was then fitted to a polynomial in V ,

$$\ln \theta_E(V, T) = \sum_{i=0}^n b_i(T) V^i, \quad (6)$$

where the logarithm of the Einstein temperature was used for numerical convenience. It transpired that above a certain temperature T_0 , the Einstein temperatures became coincident. Thus we used $\theta_E(V, T_0)$ to regenerate the *ab initio* free energy over the complete temperature range. This introduces some error at temperatures less than T_0 but avoids the interpretational difficulty associated with a temperature dependent zero point energy. The temperature independence of the Einstein temperature means that the solid equation of state can be written in the Mie-Grüneisen form with the Grüneisen function given by $\Gamma = -(d \ln \theta_e / d \ln V)$.

III. THERMODYNAMICS OF hcp MAGNESIUM

A. The variation of the c/a ratio with pressure

Recently, Errandonea *et al.*¹² measured the c/a ratio as a function of pressure and found that it was effectively constant for pressures higher than 5 GPa. These findings contradicted earlier measurements^{27,28} which found a significant

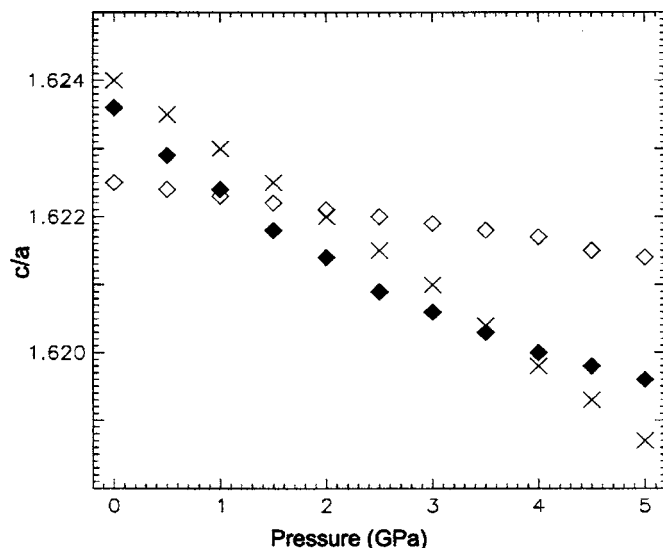


FIG. 1. Comparison of the theoretical and experimental variations of the c/a ratio of hcp Mg at low pressure. (\blacklozenge) GGA, (\diamond) LDA, and (\times) experimental data of Ref. 12.

variation with pressure. We undertook a theoretical study of the variation of the c/a ratio with pressure. The electronic energy for atomic volumes corresponding to pressures in the range of 0–55 GPa was computed. These calculations were performed using a $28 \times 28 \times 20$ k -point grid, which included the Γ point, with Brillouin zone integration performed using the tetrahedron method.²⁹ The plane wave cutoffs for the band electrons and augmentation charges were set to 350 and 1050 eV, respectively. At each volume, calculations were performed for a range of c/a values at intervals of 0.001. The c/a for each volume was then determined by fitting a second-order polynomial to the E -(c/a) data and finding the c/a value at the minimum energy.

By fitting their results to a second-order polynomial, Errandonea *et al.* found the slope of c/a at zero pressure to be $-9.3 \times 10^{-4} \text{ GPa}^{-1}$. We found that a cubic polynomial reproduced the c/a calculations reasonably well to a pressure of around 20 GPa. With these fits, we determined the slopes at zero pressure to be $(-1.6$ and $-13.7) \times 10^{-4} \text{ GPa}^{-1}$ for the LDA and GGA, respectively. The slower falloff of the LDA

TABLE I. Comparison of theoretical equilibrium structural properties of hcp magnesium at $T=0$ K with experimental RTP values. V_0 is the atomic volume, K_0 is the bulk modulus, K'_0 is its pressure derivative, and E_0 is the cohesive energy per atom.

	V_0 (\AA^3)	K_0 (GPa)	K'_0	E_0 (eV)
LDA (PAW) ^a	21.66	40.1	3.86	-1.76
LDA (PP) ^b	22.60	37.0		-1.62
LDA (GPT) ^c	22.58	32.6		-1.60
LDA (FP-LAPW) ^d	21.60	40.1		-1.48
GGA (PAW) ^a	22.97	36.0	3.88	-1.48
GGA (FP-LAPW) ^d	22.98	37.0		-1.48
Expt. ^e	23.24	36.8 ± 3	4.3 ± 0.4	-1.51

^aProjector augmented wave calculation (this work).

^bPseudopotential calculation of Ref. 31.

^cGeneralized pseudopotential calculation of Ref. 9.

^dFull potential linear augmented plane wave calculation of Ref. 32.

^e V_0 from Ref. 33, E_0 from Ref. 34, and other values from Ref. 12.

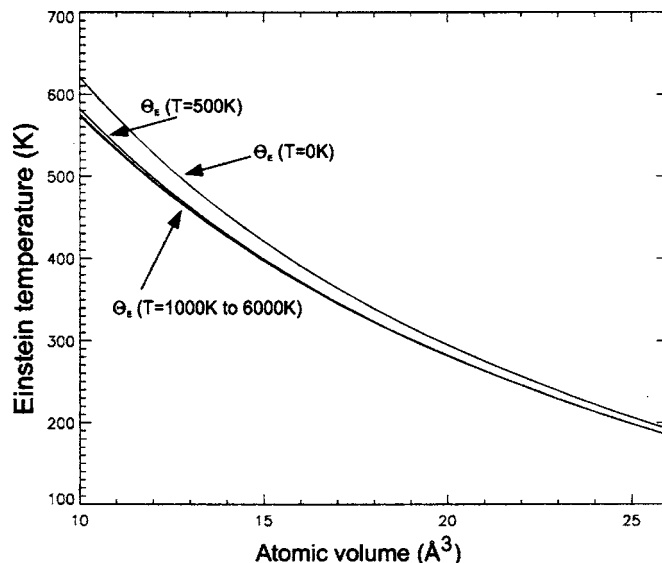


FIG. 2. The Einstein temperatures obtained from the ionic free energy of hcp Mg in the range of 0–6000 K from the GGA calculation. The $T=0$ K case represents a fit to the zero point energy only and is noticeably different. The $T=500$ K case is only just distinguishable from the the lowest curve, which are the Einstein temperatures in the range of 1000–6000 K.

c/a ratio is seen in Fig. 1, which compares the low pressure fits of the present calculations with the fit of Errandonea *et al.* These fits also determined the equilibrium values for c/a to be to be 1.6225 and 1.6236 for the LDA and GGA, respectively, which are both in excellent agreement with the experimental value of 1.624.¹² Above a pressure of ca. 10 GPa, the LDA and GGA calculations became coincident and remained constant, in agreement with the findings of Errandonea *et al.* The effective pressure independence of the c/a ratio enabled us to keep it constant at the predicted equilibrium values in further calculations; i.e., the value 1.6225 was used in the LDA calculations and the value 1.6236 was used in the GGA calculations.

TABLE II. Comparison between calculation and experiment of various properties of Mg at RTP. ρ_0 is the density, K_0 is the isothermal bulk modulus, K'_0 is its derivative with respect to pressure, C_p is the constant pressure specific heat capacity, β is the volume expansion coefficient, θ_E is the Einstein temperature, u_B is the bulk sound speed, and Γ is the thermodynamic Grüneisen parameter.

	GGA	LDA	Expt.
ρ_0 (g cm^{-3})	1.711	1.818	1.738^a
K_0 (GPa)	32.4	36.2	36.8 ± 3^b
K'_0	4.03	4.07	4.3 ± 0.4^b
C_p ($\text{kJ kg}^{-1} \text{K}^{-1}$)	1.034	1.026	1.025^c
β (10^{-5}K^{-1})	8.62	7.95	7.44^d
θ_E (K)	220	232	248^e
u_B (km s^{-1})	4.44	4.55	4.44^f
Γ	1.64	1.60	1.6^g

^aReference 33.

^bReference 12.

^cReference 35.

^dReference 36.

^eReference 37.

^fReference 38.

^gReference 9.

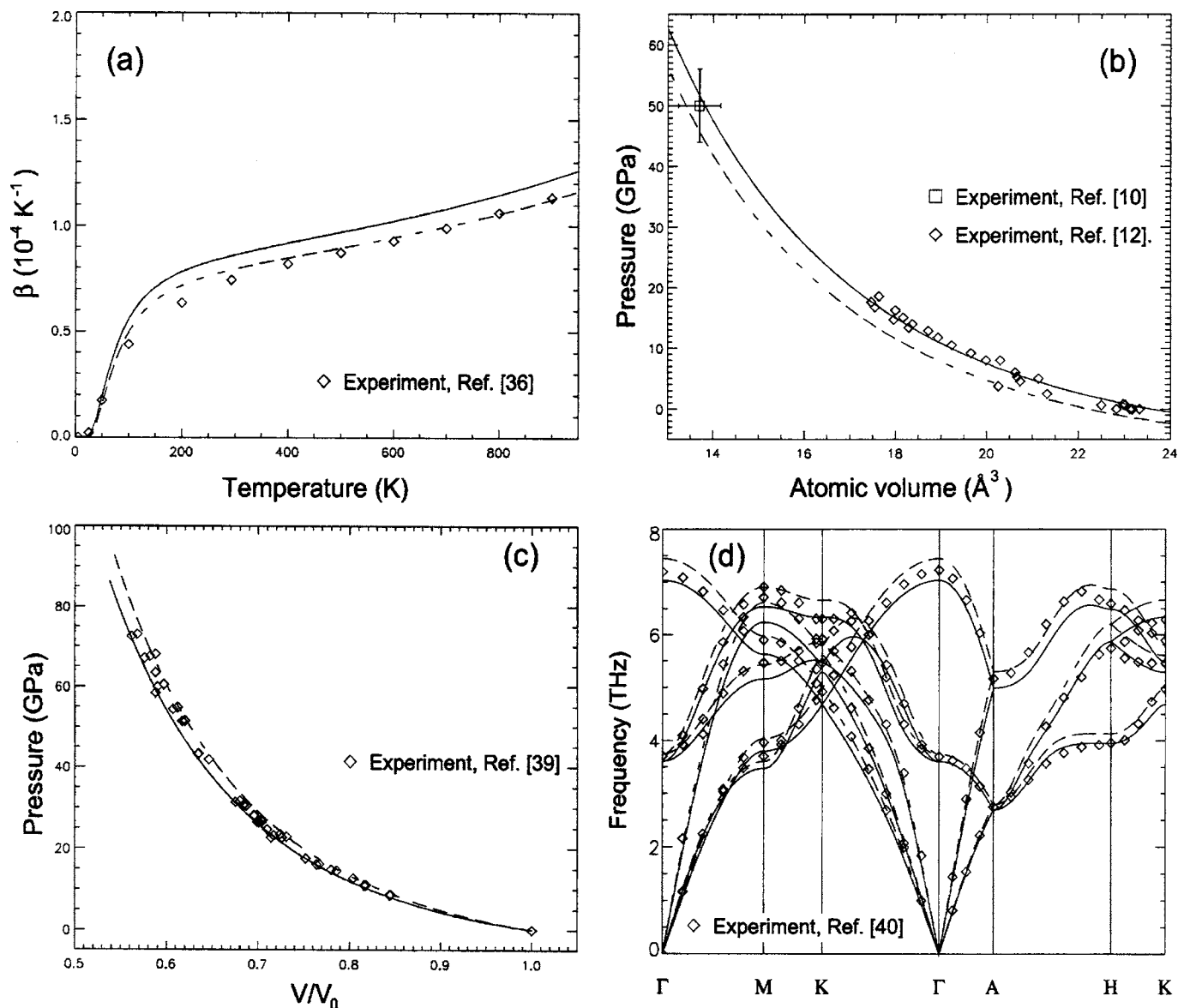


FIG. 3. Thermodynamic properties of hcp Mg [(—) GGA and (---) LDA]. (a) Volume expansion coefficient along the atmospheric isobar. (b) Room pressure isotherm. (c) Pressure along the Hugoniot. (d) Phonon dispersion at the equilibrium volume.

B. The equation of state

The electronic free energy of the static lattice was computed for atomic volumes in the range of 10–26 \AA^3 , in steps of 0.5 \AA^3 , and at electronic temperatures in the range of 0–6000 K, in steps of 100 K.³⁰ The resulting free energy isotherms were parametrized using the process described in Sec. II, with the coefficients of the Birch-Murnaghan function fitted to fourth-order polynomials in T . The fitting process generally led to the *ab initio* calculations being reproduced to less than 1 meV over most of the volume range. The 0 K values of Birch-Murnaghan parameters obtained are displayed in Table I, which also shows results obtained from other first principles calculations. In particular, we note the close agreement between our calculations and the FP-LAPW calculations of Jona and Marcus.³² This agreement demonstrates the accuracy of the PAW method, which is formally equivalent to the frozen-core all-electron approximation.

In the calculation of the ionic free energy the conver-

gence strategy detailed in Ref. 23 was followed. Test calculations were performed at a number of volumes with different sized supercells and different sized integration grids. It was found that a $3 \times 3 \times 2$ supercell, Γ -centered k -point grid of $6 \times 6 \times 6$, atomic displacement of 0.7% of the lattice parameters and a Γ -centered $12 \times 12 \times 12$ q grid, for computation of the phonon density of states, gave convergence of the mean geometric frequency $\bar{\omega}_g$ to less than 1%. To achieve this degree of convergence, it was found necessary to increase the plane wave cutoffs to 550 and 1750 eV for the valence states and augmentation charges, respectively. These calculations were performed at a number of electronic temperatures up to 2000 K. It was found that the phonon dispersion was insensitive to the electronic temperature and consequently, further calculations were performed at an electronic temperature of 300 K.

From the isothermal free energies, an Einstein temperature was determined by inversion of Eq. (5). Figure 2 shows

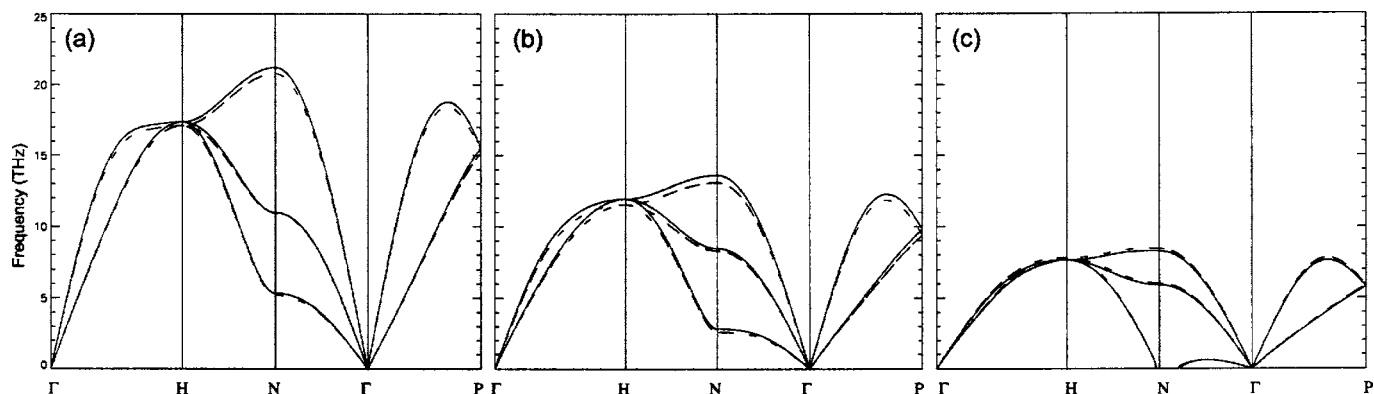


FIG. 4. The phonon dispersion of bcc Mg along the Brillouin zone symmetry directions at various atomic volumes [(—) GGA and (- - -) LDA]. (a) $V = 10 \text{ \AA}^3$, (b) $V = 15 \text{ \AA}^3$, and (c) $V = 21.5 \text{ \AA}^3$ (GGA) and $V = 20.5 \text{ \AA}^3$ (LDA).

the Einstein temperature as a function of volume for various temperatures for the GGA calculations. It is seen that above 1000 K, the Einstein temperatures become coincident. Rather than use a temperature dependent Einstein temperature, we used the Einstein temperature at 1000 K. This does introduce some error at lower temperatures, but these were found to be less than 5 meV.

Using the analytic representation of the total *ab initio* free energy, numerous thermodynamic properties were computed. Table II summarizes a number of properties at room temperature and pressure (RTP). Generally, it is seen that the agreement with experiment is good. We note, however, that the predicted LDA equilibrium density is a little high and the the GGA bulk modulus is a little low. It is interesting to note that the cold GGA value for the bulk modulus (see Table I) is in agreement with the experimental RTP value, but the inclusion of thermal effects reduce the cold value considerably. Although the GGA prediction of the bulk modulus is worse than that of the LDA, it is in line with previous findings that the GGA can overcorrect LDA values to the extent that GGA results end up being worse than the LDA value.³

A selection of various thermodynamic properties are shown in Fig. 3. The volume expansion coefficient is shown in Fig. 3(a), and it is seen that the LDA prediction is in very good agreement with experiment, with the GGA calculation being slightly higher. In their study of copper, Narasimhan and de Gironcoli⁶ found similar behavior, which they explain from the relationship $\beta = \Gamma C_v / 3K_0$. In their work, C_v and Γ were very close to the experimental values for both the LDA and GGA. They conclude that the major source of error in β originates from K_0 , for which the LDA value is in better agreement with experiment than the GGA value. We find the same pattern in this work, thus we also conclude that the excellent agreement of the LDA expansion coefficient is due to the fact that the bulk modulus is in better agreement with the experimental value than the GGA prediction.

Figures 3(b) and 3(c) show the compressional behavior of magnesium. The GGA room temperature isotherm is seen to be in good agreement with experiment; the LDA is, however, seen to underestimate the pressure. Although differences between the two calculated Hugoniot are apparent, they are both in good agreement with the experimental data of Ref. 39, which is sandwiched between the LDA and GGA results.

Figure 3(d) compares the LDA and GGA phonon dispersions at their respective predicted RTP equilibrium volumes, and it is seen that the agreement with the experiment data of Pynn and Squires⁴⁰ is generally very good. It is noted that the LDA phonon frequencies are higher than those of the GGA. This is consistent with the pattern observed by the authors of Ref. 5. They explain that this behavior is a consequence of the LDA predicting an equilibrium density that is too high, and thus the system is effectively in compression which leads to an increase in phonon frequencies with the converse being true of the GGA.

IV. THE hcp-bcc TRANSITION

The equation of state of the bcc phase was calculated in a similar fashion to that for the hcp phase: The electronic Helmholtz free energy was computed in the range of 0–6000 K at intervals of 100 K, for atomic volumes in the range of 10.0–26.0 \AA^3 at intervals of 0.5 \AA^3 , and fitted to the third-order Birch-Murnaghan equation. A $18 \times 18 \times 18$ Γ -centered k -point grid was used for both the LDA and GGA calculations. The plane wave cutoffs for the static lattice calculations were the same as for the hcp calculations. For the phonon calculations, the plane wave cutoffs were, again, increased to 550 and 1750 eV for the valence electrons and augmentation charges, respectively, and the force calculations were performed at an electronic temperature of 300 K. For these calculations, a $5 \times 5 \times 5$ supercell, Γ -point centered grids of $3 \times 3 \times 3$ and $12 \times 12 \times 12$ for the electronic and phonon Brillouin zone integrations, respectively, and an atomic displacement of 0.9% gave a convergence of $\bar{\omega}_g$ to within 1%.

As seen in Fig. 4, the GGA and LDA phonon dispersions are very similar and both predict the bcc structure to become dynamically unstable at low pressures. In the case of the GGA calculations soft modes appeared in the volume range of $21.5 \text{ \AA}^3 < V \leq 21.0 \text{ \AA}^3$ and for the LDA, softening occurred in the range of $20.5 \text{ \AA}^3 < V \leq 20.0 \text{ \AA}^3$. These volumes are similar to the value of 21.6 \AA^3 calculated by Moriarty and Althoff.¹¹

The electronic and ionic free energies were fitted to the Birch-Murnaghan and Einstein functions (using the Einstein temperature evaluated at 1000 K), respectively. These parametrizations were performed only over the volume range

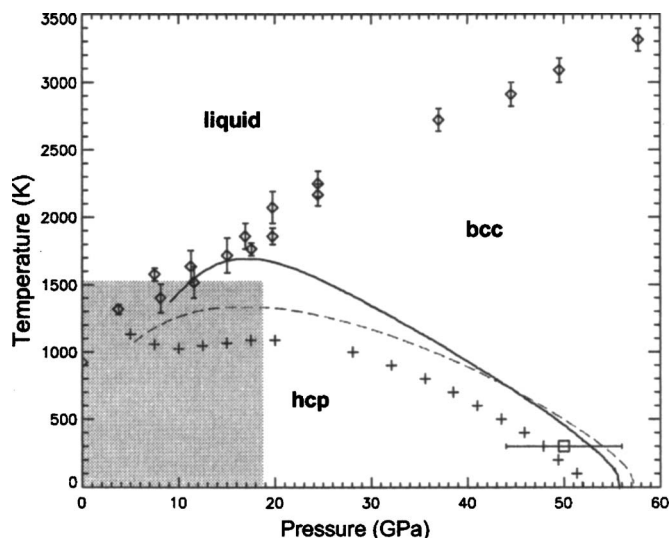


FIG. 5. Phase diagram of Mg[—] GGA and (---) LDA]. (\diamond) is the experimental melting curve of Errandonea *et al.* (Ref. 41), (\square) is the experimental hcp-bcc transition point measured by Olijnyk and Holzapfel (Ref. 10), (+) is the GPT hcp-bcc boundary calculation of Moriarty and Althoff (Ref. 11), and the shaded area represents the P - T region investigated experimentally by Errandonea *et al.* (Ref. 12) in which no evidence for the bcc phase was found.

over which the bcc phase was dynamically stable. The hcp-bcc phase was then mapped out by computing the Gibbs free energy for each phase as a function of P and T and finding the points of equality. Figure 5 shows the calculated solid phase boundaries and included, for completeness, are the melt curve measurements of Errandonea *et al.*⁴¹ The sole experimental point on the hcp-bcc is that measured by Olijnyk and Holzapfel¹⁰ who found that the transition pressure at 300 K was 50 ± 6 GPa. The LDA and GGA predictions of 54 and 53 GPa, respectively, are in very good agreement with this value. It is seen that in the region of 40–55 GPa, the LDA and GGA phase boundaries are in close agreement with each other. At pressures lower than this, the GGA transition temperature rises more quickly than those predicted by the LDA. Also shown in Fig. 5 is the GPT phase boundary calculation of Moriarty and Althoff.¹¹ It is seen that although the shape of their transition line is similar to the present LDA calculation, the transition temperatures computed by Moriarty and Althoff are lower. The shaded portion of Fig. 5 represents the (P, T) region investigated experimentally by Errandonea *et al.*¹² within which no evidence for a bcc phase was found.⁴² It is seen that the GGA calculation is in agreement with these observations and that the LDA hcp-bcc boundary is only marginally within this region. The GPT calculation, on the other hand, predicts the bcc phase to be stable within a significant portion of the experimentally investigated region. In Ref. 11 the electronic thermal excitation is omitted, and on the basis that this might account for the discrepancy between our calculation and theirs, we repeated our calculation without the electronic contribution to the free energy. However, we found that not including this led to transition temperatures that were even higher.

V. SUMMARY

In this work we have computed numerous thermodynamic properties of hcp magnesium over wide pressure and temperature ranges and compared results obtained with the LDA and GGA. For most computed thermodynamic properties it has been found that there is very little to choose between the GGA and LDA, with both giving very similar results, and in this case at least, both produce results that are in reasonable agreement with experiment. A particular exception is the room temperature pressure isotherm, for which the LDA calculation gives noticeably poorer agreement. This, however, is a consequence of the established behavior of the LDA which tends to predict lattice constants that are too small.

Previous studies on the effect of the exchange-correlation potential on solid-solid transition pressures reported that the LDA predicts much lower pressures than the GGA.^{7,8} In the present work, however, we find that the magnesium hcp-bcc phase boundaries obtained with the LDA and GGA are close to each other in the range of 40–55 GPa. At lower pressures though, the GGA predicts the transition temperature to be higher than that computed with the LDA. Both the present phase boundaries are found to be in good agreement with the available experimental data of Refs. 10 and 12.

- ¹P. Hohenberg and W. Kohn, Phys. Rev. **136**, 864 (1964).
- ²W. Kohn and L. J. Sham, Phys. Rev. **140**, 1133 (1965).
- ³Y. Juan and E. Kaxiras, Phys. Rev. B **48**, 14944 (1993).
- ⁴A. Dal Corso, A. Pasquarello, A. Baldereschi, and R. Car, Phys. Rev. B **55**, 1180 (1996).
- ⁵F. Favot and A. Dal Corso, Phys. Rev. B **60**, 11427 (1999).
- ⁶S. Narasimhan and S. de Gironcoli, Phys. Rev. B **65**, 064302 (2002).
- ⁷N. Moll, M. Bockstedte, M. Fuchs, E. Pehlke, and M. Scheffler, Phys. Rev. B **52**, 2550 (1995).
- ⁸A. Zupan, P. Blaha, K. Schwarz, and J. P. Perdew, Phys. Rev. B **58**, 11266 (1998).
- ⁹J. D. Althoff, P. B. Allen, R. M. Wentzocovitch, and J. A. Moriarty, Phys. Rev. B **48**, 13253 (1993).
- ¹⁰H. Olijnyk and W. B. Holzapfel, Phys. Rev. B **31**, 4682 (1985).
- ¹¹J. A. Moriarty and J. D. Althoff, Phys. Rev. B **51**, 5609 (1995).
- ¹²D. Errandonea, Y. Meng, D. Häussermann, and T. Uchida, J. Phys.: Condens. Matter **15**, 1277 (2003).
- ¹³P. E. Blöchl, Phys. Rev. B **50**, 17953 (1994).
- ¹⁴G. Kresse and J. Joubert, Phys. Rev. B **59**, 1758 (1999).
- ¹⁵G. Kresse and J. Furthmüller, Phys. Rev. B **54**, 11169 (1996).
- ¹⁶Y. Wang and J. P. Perdew, Phys. Rev. B **44**, 13298 (1991).
- ¹⁷J. P. Perdew, J. A. Chevary, S. H. Vosko, K. A. Jackson, M. R. Perderson, D. J. Singh, and C. Fiolhais, Phys. Rev. B **46**, 6671 (1992).
- ¹⁸D. Ceperley and B. Alder, Phys. Rev. Lett. **45**, 566 (1980).
- ¹⁹J. P. Perdew and A. Zunger, Phys. Rev. B **23**, 5048 (1981).
- ²⁰N. D. Mermin, Phys. Rev. **137**, A1441 (1965).
- ²¹G. Kresse, H. Furthmüller, and J. Hafner, Europhys. Lett. **32**, 729 (1995).
- ²²D. Alfè, program available from <http://chianti.geol.ucl.ac.uk/~dario>
- ²³D. Alfè, G. D. Price, and M. J. Gillan, Phys. Rev. B **64**, 045123 (2001).
- ²⁴L. Vočadlo and D. Alfè, Phys. Rev. B **65**, 214105 (2002).
- ²⁵D. C. Wallace, *Thermodynamics of Crystals* (Wiley, New York, 1972).
- ²⁶F. Birch, Phys. Rev. **71**, 809 (1947).
- ²⁷G. L. Clendenon and H. G. Drickamer, Phys. Rev. **135**, A1643 (1964).
- ²⁸E. A. Perez-Albuern, R. L. Clendenon, R. W. Lynch, and H. G. Drickamer, Phys. Rev. **142**, 392 (1966).
- ²⁹P. E. Blöchl, O. Jepsen, and O. K. Andersen, Phys. Rev. B **49**, 16223 (1994).
- ³⁰The $T=0$ K electronic free energy was taken to be that evaluated at $T=1$ K.
- ³¹R. M. Wentzocovitch and M. L. Cohen, Phys. Rev. B **37**, 5571 (1988).

- ³²F. Jona and P. M. Marcus, Phys. Rev. B **66**, 094104 (2002).
- ³³<http://www.webelements.com>
- ³⁴C. Kittel, *Introduction to Solid State Physics* (Wiley, New York, 1976).
- ³⁵I. Barin, *Thermochemical Data of Pure Substances* (VCH, Weinham, 1993).
- ³⁶Y. S. Touloukin, R. K. Kirby, R. E. Taylor, and P. D. Desai, *Thermophysical Properties of Matter*, The TPRC Data Series Vol. 12 (IFI/Plenum, New York, 1975).
- ³⁷P. Wilkes, *Solid State Theory in Metallurgy* (Cambridge University Press, London, 1973).
- ³⁸R. G. McQueen, S. P. Marsh, J. W. Taylor, J. N. Fritz, and W. J. Carter, in *High Velocity Impact Phenomena*, edited by R. Kinslow (Academic, New York, 1970).
- ³⁹*LASL Shock Hugoniot Data*, edited by S. P. Marsh (University of California Press, Berkeley, 1980).
- ⁴⁰R. Pynn and G. L. Squires, Proc. R. Soc. London, Ser. A **327**, 347 (1972).
- ⁴¹D. Errandonea, R. Boehler, and M. Ross, Phys. Rev. B **65**, 012108 (2001).
- ⁴²It is mentioned that Errandonea *et al.* found an evidence for a hcp-dhcp transition rather than a hcp-bcc transition and further suggested that Olijnyk and Holzapfel may have erroneously identified a hcp-dhcp transition as a hcp-bcc transition. This is presently the source of some debate (see Refs. 43 and 44).
- ⁴³H. Olijnyk, J. Phys.: Condens. Matter **16**, 8791 (2004).
- ⁴⁴D. Errandonea, J. Phys.: Condens. Matter **16**, 8795 (2004).